Materials Today Advances 16 (2022) 100320

Contents lists available at ScienceDirect

Materials Today Advances

journal homepage: www.journals.elsevier.com/materials-today-advances/

Growth mechanism and characteristics of β-Ga_2O_3 heteroepitaxailly grown on sapphire by metalorganic chemical vapor deposition

Ray-Hua Horng [a, b, *], Dong-Sing Wuu [c, **], Po-Liang Liu [d, e], Apoorva Sood [a], Fu-Gow Tarntair [a], Yu-Hsuan Chen [d], Singh Jitendra Pratap [f], Ching-Lien Hsiao [g]

[a] Institute of Electronics, National Yang Ming Chiao Tung University, Hsinchu, 30010, Taiwan
[b] Center for Emergent Functional Matter Science, National Yang Ming Chiao Tung University, Hsinchu, 30010, Taiwan
[c] Department of Applied Materials and Optoelectronic Engineering, National Chi Nan University, Nantou, 54561, Taiwan
[d] Graduate Institute of Precision Engineering, National Chung Hsing University, Taichung, 40227, Taiwan
[e] Innovation and Development Center of Sustainable Agriculture, National Chung Hsing University, Taichung, 40227, Taiwan
[f] Physics Department, Indian Institute of Technology Delhi, New Delhi, 110016, India
[g] Thin Film Physics Division, Department of Physics, Chemistry and Biology (IFM), Linköping University, SE-581 83, Linköping, Sweden

ARTICLE INFO

Article history:
Received 24 September 2022
Received in revised form
2 November 2022
Accepted 2 November 2022
Available online 7 November 2022

Keywords:
Gallium oxide
Metalorganic chemical vapor deposition
Crystalline
Roughness
Growth mechanism

ABSTRACT

In this study, monoclinic gallium oxide (β-Ga_2O_3) epilayer was successfully grown on *c*-plane, (0001), sapphire substrate by metalorganic chemical vapor deposition (MOCVD) with interplaying growth temperature, TEGa flow rate, and growth time. X-ray diffraction 2θ scans show only three narrow diffraction peaks referred to β-Ga_2O_3($\bar{2}$ 01), ($\bar{4}$ 02), and ($\bar{6}$ 03) in all epilayers, indicating a superior crystalline quality. Current-voltage (I–V) measurement reveals that these β-Ga_2O_3 films are insulating and exhibit high resistance in a range of 10^{12}–10^{14} Ω. The crystallization characteristics of the epilayers can be effectively improved with thickness through increasing TEGa flow rate and growth time, which was evidenced by X-ray rocking curves and I–V measurements. However, the surface roughness of β-Ga_2O_3 film increases with growth time and TEGa flow rate. When the growth temperature increases above 825 °C, the thickness of β-Ga_2O_3 film decreases clearly. Furthermore, it can be found that the growth rate decreased as the growth time increasing. The growth mechanism based on first-principles calculation was proposed as that 3D growth induced by the lattice mismatch between β-Ga_2O_3 and sapphire starts at nucleation stage, and follows up a lateral growth promoting a 2D growth after the thick epilayer being grown. In addition, the complex chemical reaction between TEGa and oxygen precursors was unraveled by density function theory calculation.

1. Introduction

Gallium oxide (Ga_2O_3) has several polymorphisms (including α, β, γ, δ, ε and κ) that have been reported by many researches [1–22]. The monoclinic β-Ga_2O_3 possesses the most stable crystal structure and most widely applications among these polymorphisms. Because of its superior materials properties, such as a wide bandgap (~4.9 eV), a high melting point (~1800 °C), a high breakdown electric field of 8 MV/cm, a high electron mobility of around 300 cm^2/Vs [2,3], a long-term chemical and thermal stability, nontoxicity, and ideal biocompatible properties [23–25], it has received increasing attention as a viable candidate for solar blind/UV photodetectors [3,16,19–21], high power devices [13,26], field-effect transistors [13,14], and sensors [2,23–25,27]. In particular, the extremely high critical field of β-Ga_2O_3 would provide a very high Baliga figure of merit (BFOM) up to about 3444, which yields a nearly tenfold higher than that of 4H–SiC (BFOM of 4H–SiC = 300) [15]. As compared with the high thermal budget for SiC power device processing, it is not necessary using high ion implantation temperature at 500 °C and process temperatures over 1000 °C. This indicated that the Ga_2O_3 has a high potential to instead of SiC for power device's applications.

* Corresponding author. Institute of Electronics, National Yang Ming Chiao Tung University, No. 1, University Rd., Hsinchu, 30100, Taiwan.
** Corresponding author. Department of Applied Materials and Optoelectronic Engineering, National Chi Nan University, No. 1, University Rd., Puli Township Nantou County, 54561, Taiwan.
E-mail addresses: rayhua@nycu.edu.tw (R.-H. Horng), dsw@ncnu.edu.tw (D.-S. Wuu).

https://doi.org/10.1016/j.mtadv.2022.100320

The Ga_2O_3 materials can be obtained via various methods, such as pulsed laser deposition (PLD) [4,5], magnetron sputtering [6], mist-chemical vapor deposition (mist-CVD) [7–9], vapor phase epitaxy (VPE) [10,11], molecular beam epitaxy (MBE) [12,13], metalorganic chemical vapor deposition (MOCVD) [14–16], hydrothermal processes [17,18], sol-gel [19,20], chemical bath deposition (CBD) [21,22], and so on. Among them, MOCVD is the most promising growth technology because MOCVD can be used to mass produce the epilayers.

In the past decade years, β-Ga_2O_3 had been grown on various substrates by MOCVD [28–37], such as MgO [28], Si [29], GaAs [30], $MgAl_2O_4$ [31], $SrTiO_3$ [32], β-Ga_2O_3 [33], sapphire [26,34–37]. Because the sapphire substrates possess low cost, easy to obtain, high thermal, and small mismatches in lattice and thermal expansion coefficient to β-Ga_2O_3, it was attractive more researchers to grow the Ga_2O_3 epilayer on sapphire substrate. F. Alema et al. [35] grew epitaxial β-Ga_2O_3 thin films on sapphire substrates using $Ga(DPM)_3$ (DPM, dipivaloylmethanate), triethylgallium (TEGa) and trimethylgallium (TMGa) precursors that films grown from each of the Ga sources had high growth rates. The highest growth rate can achieve to 10 μm/h using a TMGa precursor at a substrate temperature of 900 °C [35]. T. Zhang Ma et al. [36] reported high-quality β-Ga_2O_3 were heteroepitaxially grown on off-angled *c*-plane sapphire substrates following step-flow growth mode at the lower growth pressure (20–40 Torr). Grains size and growth rate decreased with the increasing growth pressure, and β–Ga_2O_3 film became more compact at higher growth pressure [37]. Moreover, the β-Ga_2O_3-based photodetectors (PDs) fabricated on 6° off-axis sapphire substrate showed excellent optical performance.

Nonetheless, there was rarely studies on the growth mechanism and the effect of growth parameters on the properties β–Ga_2O_3 hetero-epilayers grown on the *c*-plane sapphire substrate. Thermal dissociation of appropriate molar amounts of TEGa precursors react with O_2 to produce approximate transition states (TSs), which are complex chemical reactions that needs to be determined along a reaction coordinate. In this work, we therefore present a comprehensive study dedicated to the growth of high-quality monoclinic β-Ga_2O_3 epilayer on *c*-plane sapphire substrates by MOCVD in terms of varying growth parameters, such as growth time, TEGa flow rate, and temperature. The thickness, surface morphology and roughness, crystallinity, and electrical conductivity of β-Ga_2O_3/sapphire were investigated using scanning electron microscopy (SEM), atomic force microscopy (AFM), X-ray diffraction (XRD), and four-probe current-voltage (I–V) measurement, respectively. With interplaying growth parameters, β-Ga_2O_3 epilayers with greatly crystalline and high resistance properties were obtained. Furthermore, the growth mechanism and chemical reaction of precursors were discussed through modelling and simulation by First principles calculation.

2. Experimental

In this work, the β-Ga_2O_3 epilayer was grown on c-plane (0001) sapphire substrates by MOCVD. The equipment model of the used MOCVD is the remodel of THOMAS SWAN 2″x19 GaN MOCVD system and the size of the sapphire substrates were 2 inch. The TEGa and high purity O_2 (99.999%) were used as the precursors for Ga and O, respectively. High purity Ar (99.999%) was used as the carrier gas for TEGa. The O_2 flow rate and growth pressure were 500 sccm and 25 torr, respectively. Afterwards, the growth parameters were adjusted at different growth time, different TEGa flow rate, and different growth temperature. The crystal structure and orientation were determined by using X-ray diffraction (XRD, PANalytical, and X'Pert Pro MRD). In addition, the surface morphology and thickness of β-Ga_2O_3 epilayers were observed by scanning electron microscopy (SEM, JEOL JSM-7800F). The film thickness was calculated using the average from the 5 positions thickness. The root-mean-square (RMS) surface roughness of β-Ga_2O_3 epilayer was measured by atomic force microscope (AFM, Dimension 5000). Electrical conductivities were evaluated by current-voltage (I–V) measurement with four-point probe and semiconductor parameter analysis instruments.

3. Results and discussion

3.1. Grown Ga_2O_3 epilayer on sapphire at different growth temperature

It is well known that there are two kinds of growth mechanism for the MOCVD; one is kinetic and the other is mass transfer. For the first one, the growth rate depends on the growth temperature. For the mass transfer, the growth rate is independent with growth temperature. In order to obtain the relations of growth rate and growth temperature, the TEGa and O_2 flow rates were 100 and 500 sccm, respectively. The growth time was maintained at 30 min. The growth temperature was controlled at 800, 825, 850, 875 and 900 °C, respectively. Fig. 1 showed the diffraction spectra of the epilayers grown at 800, 825, 850, 875 and 900 °C. Obviously, all the epilayers presented the β-Ga_2O_3 phase. Not only, they were single crystal with ($\bar{2}$ 01), ($\bar{4}$ 02) and ($\bar{6}$ 03) diffraction planes at 18.9°, 38.3° and 59.0°, respectively. The diffraction peak (2θ) and full width of half maximum (FWHM) of ($\bar{4}$ 02) for the β-Ga_2O_3 grown at 800, 825, 850, 875 and 900 °C were shown in the inset Table of Fig. 1. It was found that the diffraction peaks of ($\bar{4}$ 02) and the corresponding FWHM were 38.35, 38.31, 38.32, 38.34, 38.35° and 0.290, 0.286, 0.284, 0.278, 0.268° for the β-Ga_2O_3 grown at 800, 825, 850, 875 and 900 °C. Obviously, there were a little different diffraction peaks for these epilayers. The FWHM of ($\bar{4}$ 02) decreased and showed the better crystallinity as the growth temperature increasing. As compared with the diffraction peak (38.437°) of ($\bar{4}$ 02) β-Ga_2O_3 (JCPDS card: No.43–1012), the peak of heteroepitxial layer showed the lower diffraction peaks. It could be resulted from the different of thermal expansion coefficients between the Ga_2O_3 and sapphire.

The thickness and growth rate of β-Ga_2O_3 epilayer as function of growth temperature were illustrated in Fig. 2. The thickness is 108, 119, 114, 101 and 95 nm for the Ga_2O_3 were grown at 800, 825, 850, 875 and 900 °C, respectively. It was found that the thickness of β-

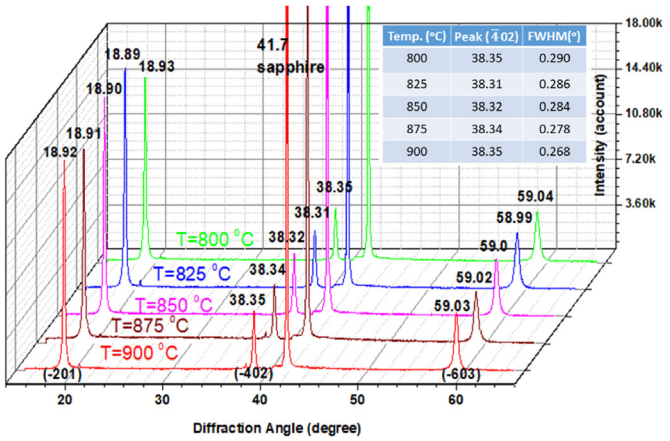

Fig. 1. Diffraction spectra of the epilayers grown at 800, 825, 850, and 900 °C. The inset table showed the ($\bar{4}$ 02) peak position and corresponding FWHM of Ga_2O_3 grown at 800, 825, 850, 875 and 900 °C.

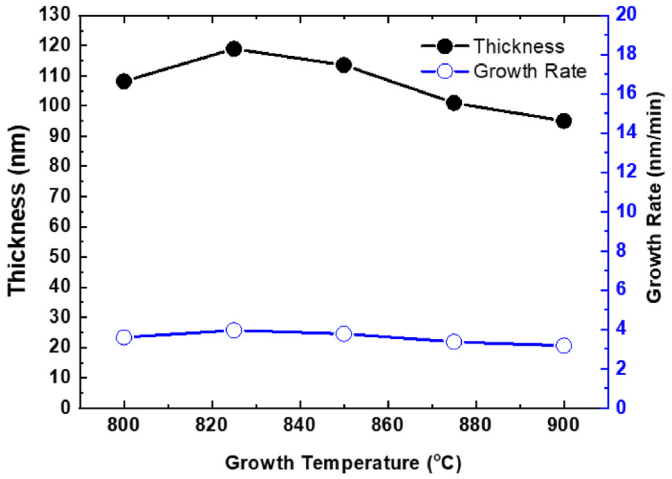

Fig. 2. Thickness and growth rate of β-Ga_2O_3 epilayer as function of growth temperature.

Ga_2O_3 increase first, then decreasing as the temperature increasing. The thickest β-Ga_2O_3 epilayer can be obtained and grown at 825 °C. After that, as the temperature increases, the thickness of the β-Ga_2O_3 epitaxial layer gradually decrease. In addition, it can be found that the growth rate is 3.6, 4.0, 3.8, 3.4 and 3.2 nm/min, respectively. It could be the kinetic domination for the Ga_2O_3 growth as the growth temperature lower than 825 °C. The growth temperature from 825 to 850 °C could be the mass transferred domination. However, it was found that the growth rate decreasing again as the growth temperature increasing (>850 °C). It could be resulted from the formation and desorption of volatile gallium suboxide, Ga_2O [9].

The surface morphology for the Ga_2O_3 grown at 800, 825, 850, and 900 °C were measured by SEM and shown in Fig. 3. Obviously, all the epilayers presented regular shaped crystals and well-defined boundaries. As the growth temperature increasing, more compact surfaces and larger regular boundaries are exhibited. These results imply an improved crystal quality with increasing the growth temperature. The obtained results are in accordance with the results of XRD. Noted that although there existed the most regular shapes crystals, it presented more steps on the surface as the epilayer grown at 900 °C. It indicates that the surface is rougher as compared those of epilayers grown at 825 and 850 °C. Because the epilayer grown at 825 °C presents the smoothest surface and preserves the highest growth rate, other parameters used in the follow-up depositions will be optimized under the 825 °C.

3.2. Grown Ga_2O_3 epilayer on sapphire at different TEGa flow rate

In general, the growth rate of the epilayer grown by MOCVD is dominated by the flow rate of metalorganic source. In order to examine the behavior for the Ga_2O_3, the TEGa flow rate was changed. The growth temperature, growth time and O_2 flow rate were maintained to be 825 °C, 60 min and 500 sccm. The β-Ga_2O_3 epilayers were grown by adjusting the TEGa flow rates to be 100, 200 and 300 sccm. According to the cross-sectional SEM image, it can be found that the thickness of β-Ga_2O_3 epilayer increases with the TEGa flow rates increasing. The thicknesses of β-Ga_2O_3 epilayer grown using TEGa flow rates of 100, 200 and 300 sccm are 216.3, 297.4 and 378.4 nm, which yields corresponding growth rates of 3.60, 4.96 and 6.31 nm/min, respectively. Fig. 4 showed the thickness and growth rate as function of TEGa flow rate. The thickness and growth rate of epilayers has a linear relation with the TEGs flow rate, which is in good agreement with the results of Ref. [38]. The obtained results indicated that the TEGa can be totally decomposed and reacted with O_2 to form the Ga_2O_3 at 825 °C.

The surface morphology and roughness of β-Ga_2O_3 grown at the different TEGa flow rate were shown in Fig. 5. The experimental results found that the surface morphology has obvious stacking phenomenon, flaky and block structure, that shown in Fig. 5(a)–(c). In addition, the high TEGa flow rates resulted in the surface

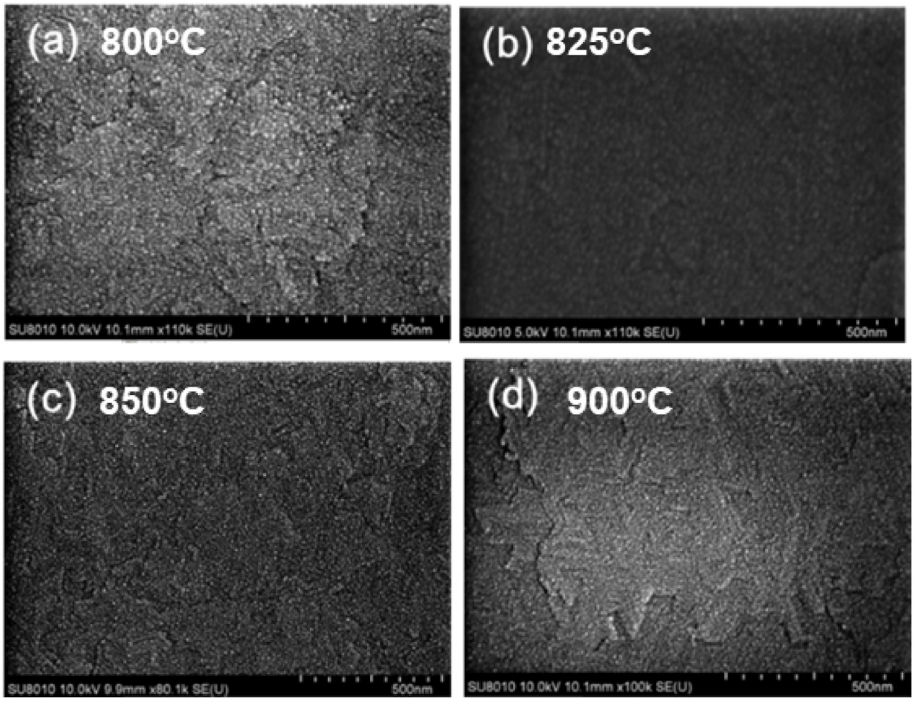

Fig. 3. Surface morphologies measured by SEM of β-Ga_2O_3 epilayer grown at (a) 800, (b) 825, (c) 850 and (d) 900 °C.

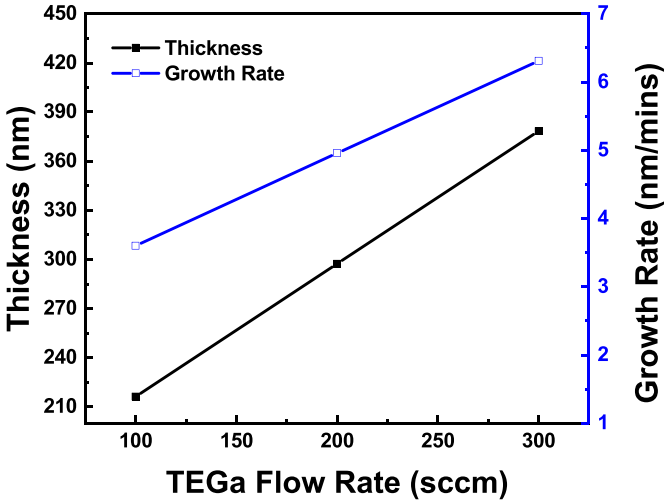

Fig. 4. Thickness and growth rate as function of TEGa flow rate. The growth temperature was 825 °C.

roughness of epilayer increasing slightly. In Fig. 5(d)–(f), the RMS of surface roughness with various TEGa flow rates of 100, 200 and 300 sccm is 6.12 nm, 7.28 nm, and 7.93 nm, respectively. Note, all these β-Ga_2O_3 films were heteroepitaxially grown on sapphire. It means that the initial growth is very important. If the growth rate was too high, it could result in the 3D growth and also result in the surface becoming rough. As concerning this point, the TEGa flow rate was not further increased for increasing growth rate.

3.3. Grown Ga_2O_3 epilayer on sapphire at different growth time

In order to understand whether the film's growth rate varies with time, various Ga_2O_3 epilayers were grown with different growth time. TEGa and O_2 flow rates were kept at 100 and 500 sccm, respectively, and the growth temperature was 825 °C. It is well known that the initial stage is very important for the epitaxial layer growth. The surface morphology of Ga_2O_3 grown with 5, 10 and 30 min were shown in Fig. 6. It was found that the Ga_2O_3 presented the islands distributed shown in Fig. 6 (a) on the sapphire substrate as the initial stage growth. As the growth time upto 10 min, the islands merged together and almost become Ga_2O_3 film, shown in Fig. 6(b). Even though, there existed some gaps in the epilayer, which were presented by red circles in Fig. 6(b). After 30 min growth, these islands totally merged together and formed the Ga_2O_3 epilayer, shown in Fig. 6(c). Thus, the growth time of 30, 60, and 120 min was controlled to evaluate the growth rate variation of β-Ga_2O_3 epilayer. The cross-section of Ga_2O_3 grown with 30, 60 and 120 min were shown in the inset of Fig. 7. The corresponding measured thickness of the MOCVD-deposited β-Ga_2O_3 epilayer were 108.13, 221.65 and 386.56 nm. The experimental results found that the thickness of β-Ga_2O_3 epilayer increases as the growth time increased. Fig. 7 shows that the thickness and growth rate of β-Ga_2O_3 film as function of growth time. Inset figures show the thickness of epilayer grown with 30–120 min measured by SEM. The β-Ga_2O_3 epitaxial layer becomes thicker as the growth time increases. The thickness of β-Ga_2O_3 films showed a tendency of linear with growth time. However, the growth rates of β-Ga_2O_3 epilayer was calculated to be3.875, 3.604 and 3.199 nm/min, respectively. It can be found that the growth rate decreased as the growth time increasing.

In Fig. 8, β-Ga_2O_3 epilayer possess three main diffraction peaks and crystalline orientations, that is, 18.91°($\bar{2}$ 01), 38.33°($\bar{4}$ 02), and 59.00°($\bar{6}$ 03) can be observed on the XRD spectra (JCPDS No.43–1012) [33,39]. Although the Ga_2O_3 grown with 5 min which presented the islands distribution, there still existed the ($\bar{2}$ 01) preferred orientation. It indicated that these thin films consisted of pure β-Ga_2O_3 and the crystalline structure with a single orientation along the ($\bar{2}$ 01) direction. Considering the effect of angle factor, ($\bar{4}$ 02) reflection was selected for rocking curve measurement (not shown the data). According to XRD spectrum, the crystalline characteristic of epilayer grown at 120 min is superior than those of grown at 60 and 30 min. It can be found that the intensity of XRD spectra and the FWHM of β-Ga_2O_3 also improved with the increase of the growth time. According to Fig. 8, the FWHM of ($\bar{4}$ 02) β-Ga_2O_3 epilayer was grown at 30, 60, and 120 min growth time is 1037, 947, and 886 arcsec, respectively. Thus, the growth time increases, the FWHM of β-Ga_2O_3 epilayer becomes narrower and the crystallinity

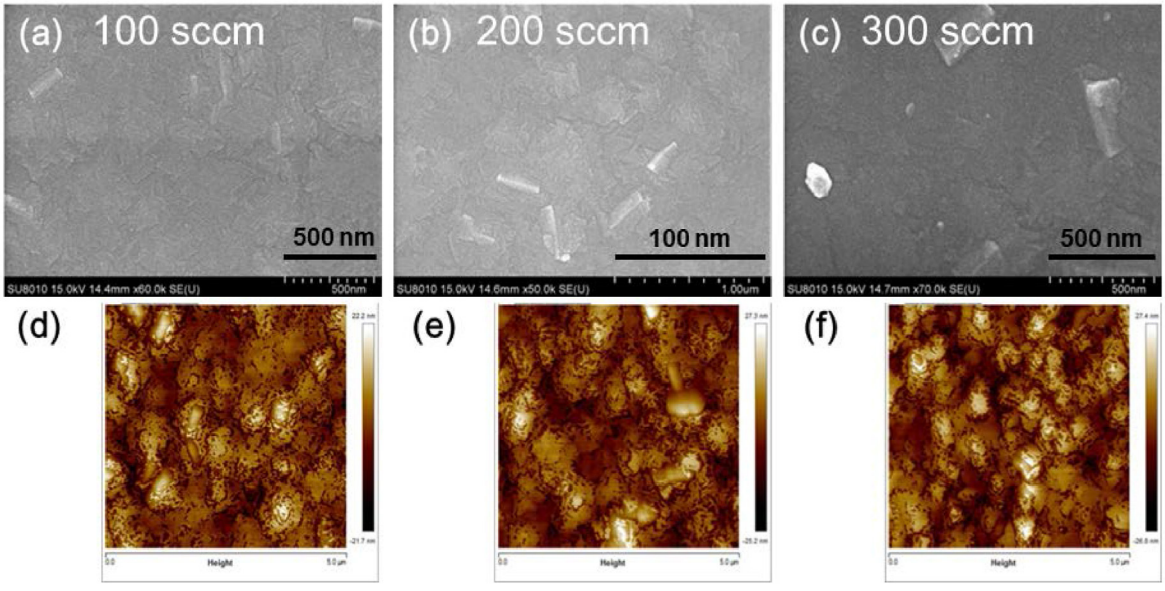

Fig. 5. Surface morphology and roughness of β-Ga_2O_3 grown at the different TEGa flow rate.

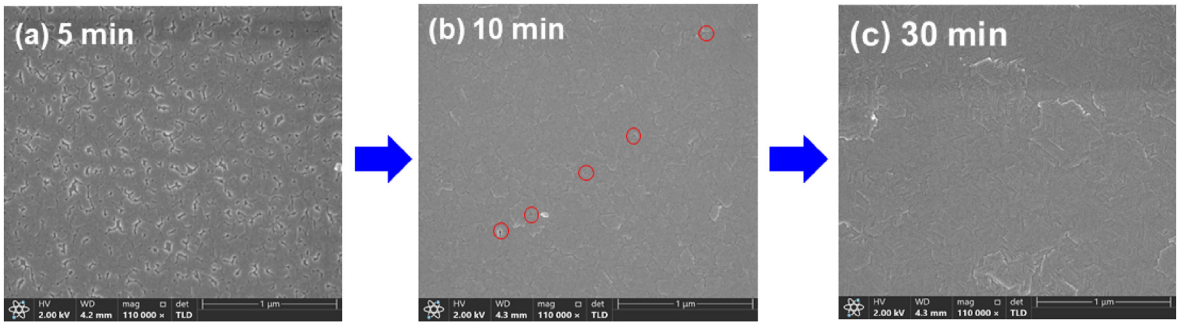

Fig. 6. Surface morphologies of Ga_2O_3 grown with (a) 5, (b) 10 and (c) 30 min.

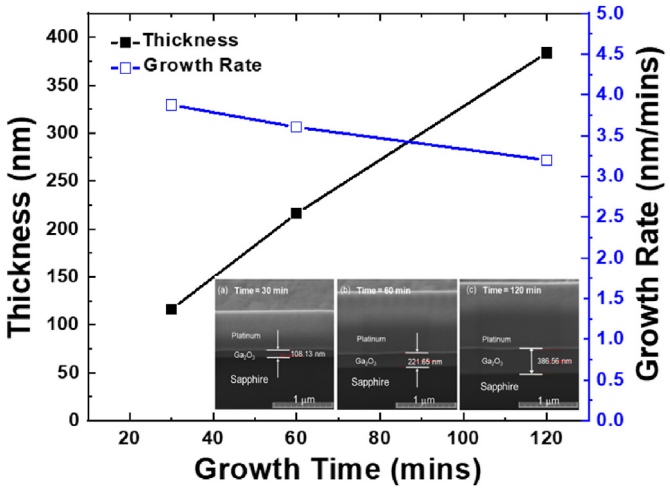

Fig. 7. Thickness and growth rate of β-Ga_2O_3 film as function of growth time. The growth temperature was 825 °C. Inset figures show the thickness measured by SEM.

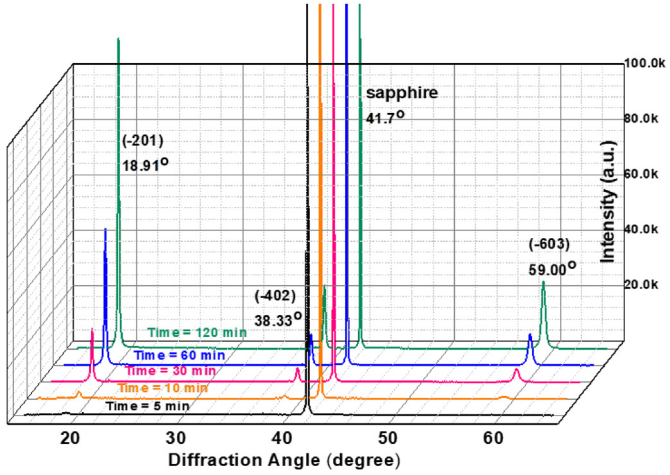

Fig. 8. Diffraction spectra of Ga_2O_3 epilayers grown with 5, 10, 30, 60 and 120 min.

characteristics of β-Ga_2O_3 becomes better. By varying the growth parameters, the crystalline quality of the films was effectively improved.

In general, the growth rate should be constant for the epitaxy growth. Due to the lattice mismatch between the β-Ga_2O_3 and sapphire, it could be 3D growth at first, then lateral growth and 2D growth after the thick epilayer being grown. The growth mechanism is proposed and the plot was shown in Fig. 9, first revealing the Volmer–Weber growth mode (3D). The 3D small islands then merge slightly together to form a two-dimensional (2D) layer structure, the so-called Frank–van der Merwe-like growth mode. Note that in the extension of 2D layers, the misfit dislocations in the films are created when the film exceeds the critical thickness. Finally, the film structures were completed by the Stranski-Krastanow growth mode consisting of 2D growth followed by the formation of 3D islands. This outcome is consistent with the observation of the initial stage growth, shown in Fig. 6 and RMS surface roughness of 4.9 nm, 6.12 nm, and 9.06 nm at the growth

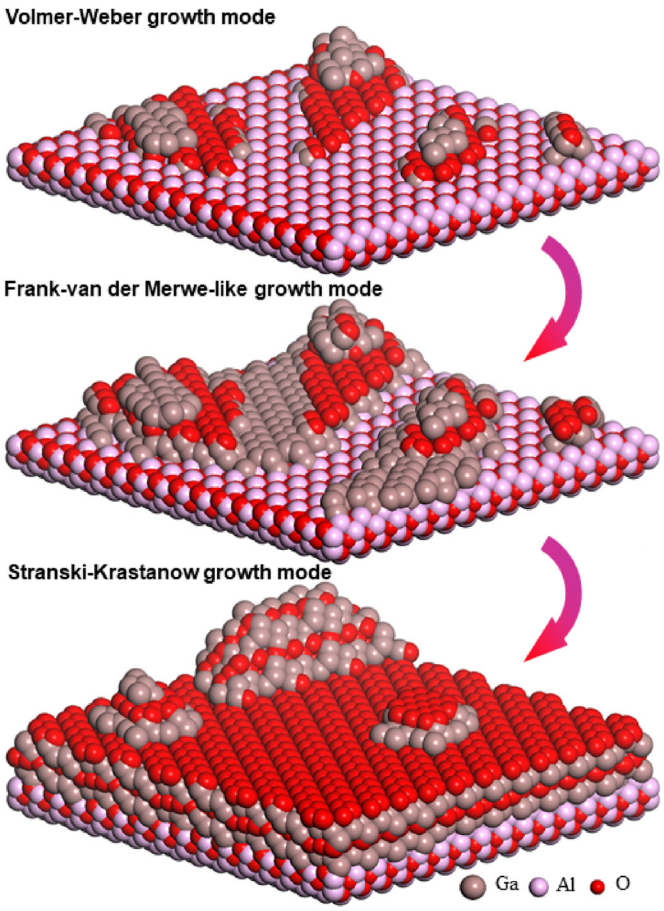

Fig. 9. Schematic diagram of the growth mechanism of β-Ga_2O_3 grown on the (0001) sapphire substrate. The atoms are represented by spheres: Ga (brown, large), Al (light-purple, medium-sized), and O (red, small). (For interpretation of the references to colour in this figure legend, the reader is referred to the Web version of this article.)

time of 30, 60, and 120 min, respectively. As increasing the growth time, surface roughness become the worst resulting the SK growth mode.

3.4. Relationship between epilayer's quality and electrical property

In addition, the electrical properties of β-Ga_2O_3 film were also measured at the above parameters. It can be seen that these as-grown β-Ga_2O_3 films exhibit high resistance characteristics in the range of 1.1×10^{13}–9.5×10^{13} Ω, as listed in Table 1. In addition, the resistance of the films decreases as the growth temperature increasing. It could be resulted from oxygen vacancy increasing as the epilayer grown at high temperature. On the other hand, the resistance increases with the growth rate and growth time as the epilayer grown at 825 °C. They were 1.5×10^{13} to 5.2×10^{13} Ω, which corresponding the resistivity 3.24×10^{8} Ω cm to 1.97×10^{9} Ω cm as growth rate from 100 sccm to 300 sccm. As the growth time increasing from 30 min to 120 min, the resistance increased from 1.5×10^{13} to 9.5×10^{13} Ω, which corresponding the resistivity 3.24×10^{8} Ω cm to 3.67×10^{9} Ω cm as growth rate from 100 sccm to 300 sccm. These indicates that the intrinsic Ga_2O_3 epilayers have high insulating properties. In addition, no matter how the experimental parameters are adjusted, the β-Ga_2O_3 films possess good crystalline structure, high resistance characteristics, all β-Ga_2O_3 films are insulating and the resistance range is about 10^{12}–10^{14} Ω.

3.5. Structures along the reaction coordinate for TEGa

The growth of β-Ga_2O_3 thin films was conducted using TEGa and O_2 as the source of Ga and O, respectively, and synthesized using MOCVD. Thermal dissociation of appropriate molar amounts of TEGa precursors react with O_2 to produce approximate transition states (TSs), which are complex chemical reactions that needs to be determined along a reaction coordinate. As a source of Ga atoms, TEGa molecules combine with O_2 to generate derivatives, such as Ga, GaO_2, GaO_4, Ga_2O_2, and Ga_2O_{10}, which are further brought to the surface of β-Ga_2O_3 by releasing ethyl groups (C_2H_5-). Note that an ethyl radical is an active molecule and two ethyl radicals could form a stable butane molecule. The proposed decomposition mechanism involves elimination of C_2H_5- as illustrated in Fig. 10. A series of density functional theory (DFT) simulations were performed to determine the structural and ground-state electronic properties of reactants and products depicted in Fig. 11. The Vienna *ab initio* simulation package was applied at the generalized gradient approximation (GGA) with the Perdew–Wang (PW91) correction [40–43] using the valence electrons of H: $1s^1$, C: $2s^2 2p^2$, O: $2s^2 2p^4$, and Ga: $4s^2 4p^1$ in all reactions. The reaction energies ΔE can be obtained by using the ground state energies of reactants and products. Based on the reaction energies ΔE of decomposition reactions of TEGa in Fig. 10, the favorable equations in terms of magnitude follow the order:

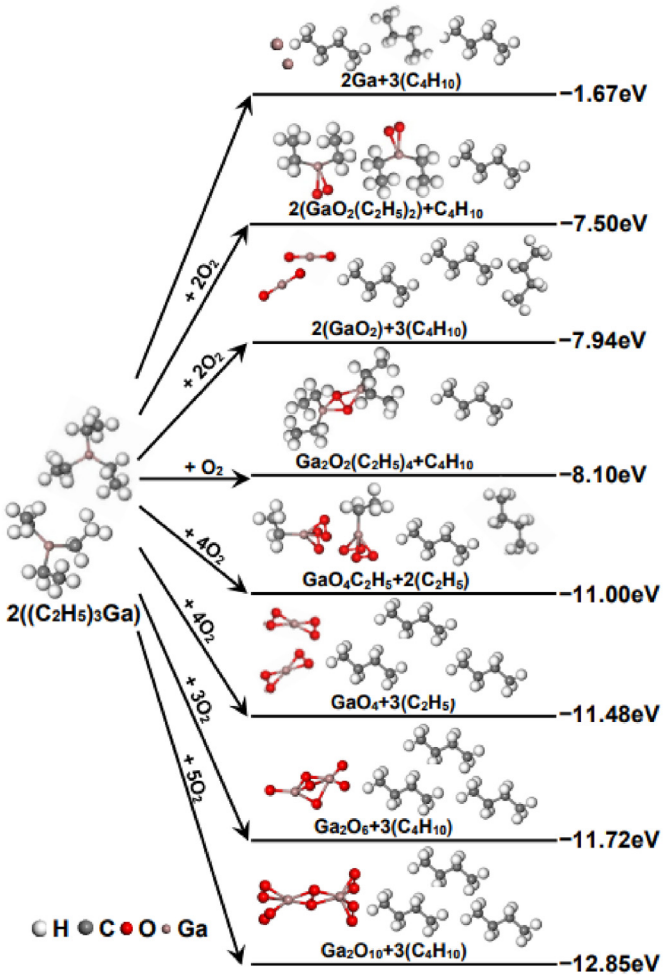

Fig. 10. Decomposition reaction of $Ga(C_2H_5)_3$ showing structural models of reactants and products. Values indicate the reaction energies ΔE (eV). The atoms are represented by spheres: H (white, large), C(gray, large), O (red, middle), and Ga (brown, small). (For interpretation of the references to colour in this figure legend, the reader is referred to the Web version of this article.)

$$2(Ga(C_2H_5)_3) \rightarrow 2Ga + 3(C_4H_{10})\ \Delta E = -1.67 \quad (1)$$

Table 1
Electrical properties of β-Ga_2O_3 films were grown at various growth parameters.

TEGa Flow Rate: 100 sccm, Growth Time: 30 min				
Growth Temp (°C)	800	825	850	900
Resistance (Ω)	1.3×10^{13}	1.5×10^{13}	9.5×10^{12}	7.6×10^{12}
Resistivity (Ω.cm)	1.40×10^{8}	1.78×10^{8}	1.08×10^{8}	8.89×10^{7}
Growth Temp: 825°C, Growth Time: 60 min				
TEGa Flow Rate (sccm)	100	200	300	
Resistance (Ω)	1.5×10^{13}	1.7×10^{13}	5.2×10^{13}	
Resistivity (Ω.cm)	3.24×10^{8}	5.06×10^{8}	1.97×10^{9}	
TEGa Flow Rate: 100 sccm, Growth Temp: 825°C				
Growth Time (min)	30	60	120	
Resistance (Ω)	1.5×10^{13}	2.1×10^{13}	9.5×10^{13}	
Resistivity (Ω.cm)	1.78×10^{8}	4.66×10^{8}	3.67×10^{9}	

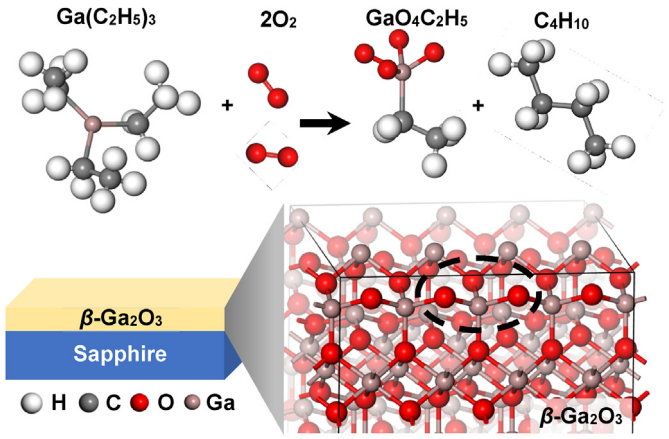

Fig. 11. Schematic illustration of the proposed β-Ga_2O_3 epitaxial layers grown on sapphire substrates. The enlarged view indicates fourfold-coordinated Ga with four O–Ga bonds embedded within the β-Ga_2O_3 thin films denoted by a dotted circle. This outcome is consistent with theoretical simulations of a decomposition reaction of $Ga(C_2H_5)_3$ involving interlinking transition states of $GaO_4C_2H_5$ and O_2 molecules. The atoms are represented by spheres: H (white, large), C(gray, large), O (red, middle), and Ga (brown, small). (For interpretation of the references to colour in this figure legend, the reader is referred to the Web version of this article.)

$$2(Ga(C_2H_5)_3) + 2O_2 \rightarrow 2(GaO_2(C_2H_5)_2) + C_4H_{10}\ \Delta E = -7.50 \quad (2)$$

$$2(Ga(C_2H_5)_3) + 2O_2 \rightarrow 2(GaO_2) + 3(C_4H_{10})\ \Delta E = -7.94 \quad (3)$$

$$2(Ga(C_2H_5)_3) + O_2 \rightarrow Ga_2O_2(C_2H_5)_4 + C_4H_{10}\ \Delta E = -8.10 \quad (4)$$

$$2(Ga(C_2H_5)_3) + 4O_2 \rightarrow 2(GaO_4C_2H_5) + 2(C_4H_{10})\ \Delta E = -11.00 \quad (5)$$

$$2(Ga(C_2H_5)_3) + 4O_2 \rightarrow 2(GaO_4) + 3(C_4H_{10})\ \Delta E = -11.49 \quad (6)$$

$$2(Ga(C_2H_5)_3) + 3O_2 \rightarrow Ga_2O_6 + 3(C_4H_{10})\ \Delta E = -11.72 \quad (7)$$

$$2(Ga(C_2H_5)_3) + 5O_2 \rightarrow Ga_2O_{10} + 3(C_4H_{10})\ \Delta E = -12.85 \quad (8)$$

Our results show Ga_2O_{10} molecules consisted of six O–Ga bonds have the lowest overall energy in Eq. (8), which closely matches the sixfold-coordinated Ga with six O–Ga bonds in the bulk of β-Ga_2O_3. Equations (5)–(7) indicate that $GaO_4C_2H_5$, GaO_4, and Ga_2O_6 molecules consisted of four O–Ga bonds are the second energetically favorable configurations, respectively, which are very similar to the fourfold-coordinated Ga with four O–Ga bonds in the bulk of β-Ga_2O_3. The other three molecules, i.e., $GaO_2(C_2H_5)_2$, GaO_2, and $Ga_2O_2(C_2H_5)_4$ in Eqs. (2)–(4), respectively, are the same higher reaction energy with the twofold-coordinated Ga with two O–Ga bonds, do not exhibit in the bulk of β-Ga_2O_3. In Eq. (1), a triethylgallium pulls ethyl groups away from the growth front, leaving pure Ga and providing Ga sources of β-Ga_2O_3, which is unfavorable in all cases. In the high-temperature regime, we speculate that highly reactive pure Ga readily nucleates through the facile reaction of O_2 to form gallium oxide, which is consistent with a significant increase of film roughness observed above about 825 °C and the morphologies of Ga_2O_3 grown with 5, 10 and 30 min, shown in Fig. 6. Furthermore, in the low-temperature regime, the low-reactivity Ga_2O_{10} molecules adsorb from the growth front and limit lateral diffusion, thereby promoting layer-by-layer growth. The nucleation on the β-Ga_2O_3 surfaces with TEGa and oxide molecules is the assembly of the proposed product structures via interlinking $GaO_4C_2H_5$, GaO_4, Ga_2O_6, or Ga_2O_{10} molecules. The plausible model described by Eq. (5) is consistent with the presence fourfold-coordinated Ga with four O–Ga bonds in the bulk of β-Ga_2O_3 as shown in Fig. 11. In general, the growth of β-Ga_2O_3 thin films composed of the GaO_6 octahedra and the GaO_4 tetrahedral would be required to release energy from the transition states of the TEGa decomposition reactions, in agreement with the evidence of the bonding arrangements of the bulk of β-Ga_2O_3.

4. Conclusions

We have grown epitaxial β-Ga_2O_3 films on the (0001) sapphire substrate through manipulating different parameters by MOCVD. The important experimental results can be summarized as the followings: i) All β-Ga_2O_3 films possess excellent quality crystalline structure. ii) These films are insulating with a resistance range of 10^{12}–10^{14} Ω iii) The thickness and surface roughness of epitaxial β-Ga_2O_3 films increases with increasing growth time and TEGa flow rate while the film growth rate decreases slightly with increasing growth time. iv) The growth rate is more sensitive to the deposition temperature above 825 °C. In addition, we proposed a three-step growth mechanism to elucidate the heteroepitaxy of β-Ga_2O_3 film on *c*-plane sapphire. The complex chemical reaction between TEGa and oxygen precursors was unraveled by density function theory calculation. This work reveals the remarkable advantages of β-Ga_2O_3 grown on sapphire substrates by MOCVD technology and provides a significant reference for boosting the performance of electronic devices application.

Credit author statement

Ray-Hua Horng: Conceptualization, Investigation, Writing –– review & editing, Supervision, Funding acquisition. Dong-Sing Wuu: Investigation, Electrical Characteristic Analyzing. Po Liang Liu: Simulation, Validation, Writing – review & editing. Apoorva Sood: Methodology, Visualization. Fu-Gow Tarntair: Epilayer Growth. Yu-Hsuan Chen: Simulation. Singh Jitendra Pratap: Crystallization Measurement. Ching-Lien Hsiao: Crystalline Quality Analyzation.

Declaration of competing interest

The authors declare that they have no known competing financial interests or personal relationships that could have appeared to influence the work reported in this paper.

Data availability

No data was used for the research described in the article.

Acknowledgment

This work was supported by the Ministry of Science and Technology (Taiwan, R.O.C.) under Grant Nos. MOST111-2923-E-A49-003-MY3, 110-2218-E-A49-020–MBK, 110-2622-8-009-018-SB, 109-2224-E-A49-003, 109-2221-E-009-143-MY3, 109-2811-E-005-508-MY2 and MOST 108-2221-E-005-028-MY3. The authors also wish to express their sincere gratitude for the financial support by the "Innovation and Development Center of Sustainable Agriculture" from The Featured Areas Research Center Program within the framework of the Higher Education Sprout Project by the Ministry of Education (MOE) in Taiwan. The authors acknowledge STINT Foundation, Sweden, for supporting this international collaboration (grant Number MG2019-8485). In addition, authors thank the Advanced Semiconductor Technology and Component Laboratory of the Institute of Electronics, National Yang Ming Chiao Tung University. We acknowledge MAtek, for funding and material measurement supporting (grant number: 2021-T-006). We also

thank Taiwan Semiconductor Research Institute (TSRI) for the processing facility supporting.

References

[1] R. Roy, V.G. Hill, E.F. Osborn, Polymorphism of Ga2O3 and the system Ga2O3−H2O, J. Am. Chem. Soc. 74 (1952) 719−722, https://doi.org/10.1021/ja01123a039.

[2] S.J. Pearton, J. Yang, P.H. Cary, F. Ren, J. Kim, M.J. Tadjer, M.A. Mastro, A review of Ga_2O_3 materials, processing, and devices, Appl. Phys. Rev. 5 (1) (2018), 011301, https://doi.org/10.1063/1.5006941.

[3] X. Chen, F. Ren, S. Gu, J. Ye, Review of gallium-oxide-based solar-blind ultraviolet photodetectors, Photon. Res. 7 (4) (2019) 381−415, https://doi.org/10.1364/PRJ.7.000381.

[4] F.B. Zhang, K. Saito, T. Tanaka, M. Nishio, Q.X. Guo, Structural and optical properties of Ga_2O_3 films on sapphire substrates by pulsed laser deposition, J. Cryst. Growth 387 (2014) 96−100.

[5] C.X. Xu, H. Liu, X.H. Pan, Z.Z. Ye, Growth and characterization of Si-doped beta-Ga_2O_3 films by pulsed laser deposition, Opt. Mater. 108 (2020), 110145, https://doi.org/10.1016/j.optmat.2020.110145.

[6] S. Mobtakeri, Y. Akaltun, A. Ozer, M. Kilic, E.S. Tuzemen, E. Gur, Gallium oxide films deposition by rf magnetron sputtering; a detailed analysis on the effects of deposition pressure and sputtering power and annealing, Ceram. Int. 47 (2021) 1721−1727, https://doi.org/10.1016/j.ceramint.2020.08.289.

[7] D. Shinohara, S. Fujita, Heteroepitaxy of corundum-structured α-Ga2O3 thin films on α-Al2O3 substrates by ultrasonic mist chemical vapor deposition, Jpn. J. Appl. Phys. 47 (2008) 7311, https://doi.org/10.1143/JJAP.47.7311.

[8] T. Kawaharamura, G.T. Dang, M. Furuta, Successful growth of conductive highly crystalline Sn-doped α-Ga2O3 thin films by fine-channel mist chemical vapor deposition, Jpn. J. Appl. Phys. 51 (2012), 040207.

[9] R. Jinno, K. Kaneko, S. Fujita, Thermal stability of alpha-Ga_2O_3 films grown on c-plane sapphire substrates via mist-CVD, AIP Adv. 10 (2021), 115013, https://doi.org/10.1063/5.0020464.

[10] Y. Yao, S. Okur, L.A. Lyle, G.S. Tompa, T. Salagaj, N. Sbrockey, R.F. Davis, L.M. Porter, Growth and characterization of α-, β-, and ε-phases of Ga2O3 using MOCVD and HVPE techniques, Mater. Res. Lett. 6 (2018) 268−275, https://doi.org/10.1080/21663831.2018.1443978.

[11] H. Murakami, K. Nomura, K. Goto, K. Sasaki, K. Kawara, Q.T. Thieu, R. Togashi, Y. Kumagai, M. Higashiwaki, A. Kuramata, Homoepitaxial growth of β-Ga2O3 layers by halide vapor phase epitaxy, APEX 8 (2014), 015503, https://doi.org/10.7567/APEX.8.015503.

[12] P. Mazzolini, P. Vogt, R. Schewski, C. Wouters, M. Albrecht, O. Bierwagen, Faceting and metal-exchange catalysis in (010) beta-Ga_2O_3 thin films homoepitaxially grown by plasma-assisted molecular beam epitaxy, Apl. Mater. 7 (2019), 022511, https://doi.org/10.1063/1.5054386.

[13] M. Higashiwaki, K. Sasaki, A. Kuramata, T. Masui, S. Yamakoshi, Development of gallium oxide power devices, Phys. Status Solidi A 211 (1) (2014) 21−26, https://doi.org/10.1002/pssa.201330197.

[14] J.H. Park, R. McClintock, M. Razeghi, Ga_2O_3 metal-oxide-semiconductor field effect transistors on sapphire substrate by MOCVD, Semicond. Sci. Technol. 34 (2019), 08LT01, https://doi.org/10.1088/1361-6641/ab2c17.

[15] J. Lee, H. Kim, L. Gautam, K. He, X. Hu, V.P. Dravid, M. Razeghi, Study of phase transition in MOCVD grown Ga2O3 from κ to β phase by ex situ and in situ annealing, Photonics 8 (2021), https://doi.org/10.3390/photonics8010017, 17.

[16] Y.S. Zhi, W.Y. Jiang, Z. Liu, Y.Y. Liu, X.L. Chu, J.H. Liu, S. Li, Z.Y. Yan, Y.H. Wang, P.G. Li, High-responsivity solar-blind photodetector based on MOCVD-grown Si-doped β-Ga2O3 thin film, Chin. Phys. B, 30, 021, 057301https://doi.org/10.1088/1674-1056/abe37a.

[17] L.S. Reddy, Y.H. Ko, J.S. Yu, Hydrothermal synthesis and photocatalytic property of β-Ga2O3 nanorods, Nanoscale Res. Lett. 10 (2015) 364, https://doi.org/10.1186/s11671-015-1070-5.

[18] H.J. Bae, T.H. Yoo, Y. Yoon, I.G. Lee, J.P. Kim, B.J. Cho, W.S. Hwang, High-aspect ratio β-Ga203 nanorods via hydrothermal synthesis, Nanomaterials 8 (2018), https://doi.org/10.3390/nano8080594, 594, 1−10.

[19] M. Yu, C.D. Lv, J.G. Yu, Y.M. Shen, L. Yuan, J.C. Hu, S.N. Zhang, H.J. Cheng, Y.M. Zhang, R.X. Jia, High-performance photodetector based on sol-gel epitaxially grown alpha/beta Ga_2O_3 thin films, Mater. Today Commun. 25 (2020), 101532, https://doi.org/10.1016/j.mtcomm.2020.101532.

[20] Y. Kokubun, K. Miura, F. Endo, S. Nakagomi, Sol-gel prepared β-Ga203 thin films for ultraviolet photodetectors, Appl. Phys. Lett. 90 (2007), 031912, https://doi.org/10.1063/1.2432946.

[21] C.Y. Yeh, Y.M. Zhao, H. Li, F.P. Yu, S. Zhang, D.S. Wuu, Growth and photocatalytic properties of gallium oxide films using chemical bath deposition, Crystals 9 (2019), https://doi.org/10.3390/cryst9110564, 564, 1−9.

[22] G. Hector, E. Appert, E. Sarigiannidou, E. Matheret, H. Roussel, O.C. Pluchery, V. Consonni, Chemical synthesis of β-Ga2O3 microrods on silicon and its dependence on the gallium nitrate concentration, Inorg. Chem. 59 (2020) 15696−15706, https://doi.org/10.1021/acs.inorgchem.0c02069.

[23] Y.L. Wu, S.P. Chang, S.J. Chang, W.Y. Weng, Y.H. Lin, A novel pH sensor using extended-gate field-effect transistors with Ga_2O_3 nanowires fabricated on SiO_2/Si template, Sci. Adv. Mater. 7 (2015) 475−478, https://doi.org/10.1166/sam.2015.1992.

[24] T. Rahman, T. Masui, T. Ichiki, Single-crystal gallium oxide-based biomolecular modified diode for nucleic acid sensing, Jpn. J. Appl. Phys. 54 (2015), 04DL08, https://doi.org/10.7567/JJAP.54.04DL08, 1−6.

[25] G. Korotcenkov, B.K. Cho, Metal oxide composites in conductometric gas sensors: achievements and challenges, Sens. Actuators, B 244 (2017) 182−210, https://doi.org/10.1016/j.snb.2016.12.117.

[26] R. Miller, F. Alema, A. Osinsky, Epitaxial β-Ga2O3 and β-(AlxGa1−x)2O3/β-Ga2O3 heterostructures growth for power electronics, IEEE Trans. Semicond. Manuf. 31 (4) (2018) 467−474.

[27] R. Pandeeswari, B.G. Jeyaprakash, High sensing response of β-Ga2O3 thin film towards ammonia vapours: influencing factors at room temperature, Sens. Actuators, B 195 (2014) 206−214, https://doi.org/10.1016/j.snb.2014.01.025.

[28] W. Mi, J. Man, Z. Zhu, C. Luan, Y. Lv, H. Xiao, Epitaxial growth of Ga_2O_3 thin films on MgO (110) substrate by metal-organic chemical vapor deposition, J. Cryst. Growth 354 (2012) 93−97, https://doi.org/10.1016/j.jcrysgro.2012.06.022.

[29] S. Schulz, G. Bendt, W. Assenmacher, D. Sager, G. Bacher, Low-temperature MOCVD of crystalline Ga_2O_3 nanowires using $^tBu_3Ga$, Chem. Vap. Depos. 19 (2013) 347−354, https://doi.org/10.1002/cvde.201307060.

[30] Y. Chen, H. Liang, X. Xia, R. shen, Y. Liu, Y. Luo, G. Du, Effect of growth pressure on the characteristics of β-Ga2O3 films grown on GaAs (100) substrates by MOCVD method, Appl. Surf. Sci. 325 (2015) 258−261, https://doi.org/10.1016/j.apsusc.2014.11.074.

[31] W. Mi, Z. Li, C. Luan, H. Xiao, C. Zhao, J. Ma, Transparent conducting tin-doped Ga_2O_3 films deposited on $MgAl_2O_4$ (100) substrates by MOCVD, Ceram. Int. 41 (2015) 2572−2575, https://doi.org/10.1016/j.ceramint.2014.11.004.

[32] D. Wang, L. He, Y. Le, X. Feng, C. Luan, H. Xiao, J. Ma, Characterization of single crystal β-Ga2O3 films grown on SrTiO3 (100) substrates by MOCVD, Ceram. Int. 46 (2020) 4568−4572, https://doi.org/10.1016/j.ceramint.2019.10.185.

[33] Z. Li, T. Jiao, J. Yu, D. Hu, Y. Lv, W. Li, X. Dong, B. Zhang, Y. Zhang, Z. Feng, G. Li, G. Du, Single crystalline β-Ga2O3 homoepitaxial films grown by MOCVD, Vacuum 178 (2020), https://doi.org/10.1016/j.vacuum.2020.109440, 109440.

[34] X. Feng, Z. Li, W. Mi, J. Ma, Effect of annealing on the properties of Ga2O3:Mg films prepared on α-Al2O3 (0001) by MOCVD, Vacuum 124 (2016) 101−107, https://doi.org/10.1016/j.vacuum.2015.06.032.

[35] F. Alema, B. Hertog, A. Osinsky, P. Mukhopadhyay, M. Toporkov, W.V. Schoenfeld, Fast growth rate of epitaxial β-Ga2O3 by close coupled showerhead MOCVD, J. Cryst. Growth 475 (2017) 77−82, https://doi.org/10.1016/j.jcrysgro.2017.06.001.

[36] T. Zhang, Z. Hu, Y. Li, Y. Zhang, Q. Feng, J. Ning, C. Zhang, J. Zhang, Y. Hao, Investigation on the β-Ga2O3 deposited on off-angled sapphire (0001) substrates, J. Lumin. 233 (2021), https://doi.org/10.1016/j.jlumin.2021.117928, 117928.

[37] T. Zhang, Y. Li, Q. Feng, Y. Zhang, J. Ning, C. Zhang, J. Zhang, Y. Hao, Effects of growth pressure on the characteristics of the β-Ga2O3 thin films deposited on (0001) sapphire substrates, Mater. Sci. Semicond. Process. 123 (2021), https://doi.org/10.1016/j.mssp.2020.105572, 105572.

[38] K. Matsuzaki, H. Hiramatsu, K. Nomura, H. Yanagi, T. Kamiya, M. Hirano, H. Hosono, Growth, structure and carrier transport properties of Ga_2O_3 epitaxial film examined for transparent field-effect transistor, Thin Solid Films 496 (2006) 37−41, https://doi.org/10.1016/j.tsf.2005.08.187.

[39] N.M. Sbrockey, T. Salagaj, E. Coleman, G.S. Tompa, Y. Moon, M.S. Kim, Large-area MOCVD growth of Ga_2O_3 in a rotating disc reactor, J. Electron. Mater. 44 (5) (2015) 1357−1360, https://doi.org/10.1007/s11664-014-3566-7.

[40] G. Kresse, J. Furthmüller, Efficiency of ab initio total energy calculations for metals and semiconductors using a plane-wave basis set, Comput. Mater. Sci. 6 (1996) 15−50, https://doi.org/10.1016/0927-0256(96)00008-0.

[41] G. Kresse, J. Furthmüller, Efficient iterative schemes for ab initio total-energy calculations using a plane-wave basis set, Phys. Rev. B 54 (1996) 11169−11186, https://doi.org/10.1103/PhysRevB.54.11169.

[42] G. Kresse, J. Hafner, Norm-conserving and ultrasoft pseudopotentials for first-row and transition elements, J. Phys. Condens. Matter 6 (1994) 8245−8257, https://doi.org/10.1088/0953-8984/6/40/015.

[43] John P. Perdew, Yue Wang, Accurate and simple density functional for the electronic exchange energy: generalized gradient approximation, Phys. Rev. B 33 (1986) 8800−8802, https://doi.org/10.1103/PhysRevB.33.8800.